A Versatile Activatable Fluorescence Probing Platform for Cancer Cells in Vitro and in Vivo Based on Self-Assembled Aptamer/Carbon Nanotube Ensembles

ARTICLE *in* ANALYTICAL CHEMISTRY · AUGUST 2014

Impact Factor: 5.64 · DOI: 10.1021/ac5024149 · Source: PubMed

9 AUTHORS, INCLUDING:

Xiaoxiao He
Hunan University
150 PUBLICATIONS **3,712** CITATIONS
SEE PROFILE

Mian Chen
Hunan University
13 PUBLICATIONS **103** CITATIONS
SEE PROFILE

Xiaosheng ye
Hunan University
13 PUBLICATIONS **206** CITATIONS
SEE PROFILE

analytical chemistry

Article

pubs.acs.org/ac

A Versatile Activatable Fluorescence Probing Platform for Cancer Cells *in Vitro* and *in Vivo* Based on Self-Assembled Aptamer/Carbon Nanotube Ensembles

Lv'an Yan,[†] Hui Shi,[†] Xiaoxiao He,* Kemin Wang,* Jinlu Tang, Mian Chen, Xiaosheng Ye, Fengzhou Xu, and Yanli Lei

State Key Laboratory of Chemo/Biosensing and Chemometrics, College of Chemistry and Chemical Engineering, College of Biology, Hunan University, Key Laboratory for Bio-Nanotechnology and Molecular Engineering of Hunan Province, Changsha 410082, China

Supporting Information

ABSTRACT: Activatable aptamer probes (AAPs) have emerged as a promising strategy in cancer diagnostics, but existing AAPs remain problematic due to complex design and synthesis, instability in biofluids, or lack of versatility for both *in vitro* and *in vivo* applications. Herein, we proposed a novel AAP strategy for cancer cell probing based on fluorophore-labeled aptamer/single-walled carbon nanotube (F-apt/SWNT) ensembles. Through π-stacking interactions and proximity-induced energy transfer, F-apt/SWNT with quenched fluorescence spontaneously formed in its free state and realized signal activation upon targeting surface receptors of living cells. As a demonstration, Sgc8c aptamer was used for *in vitro* analysis and *in vivo* imaging of CCRF-CEM cancer cells. It was found that self-assembled Cy5-Sgc8c/SWNT held robust stability for biological applications, including good dispersity in different media and ultralow fluorescence background persistent for 2 h in serum. Flow cytometry assays revealed that Cy5-Sgc8c/SWNT was specifically activated by target cells with dramatic fluorescence elevation and showed improved sensitivity with as low as 12 CCRF-CEM cells detected in mixed samples containing ~100 000 nontarget cells. *In vivo* studies confirmed that specifically activated fluorescence was imaged in CCRF-CEM tumors, and compared to "always on" probes, Cy5-Sgc8c/SWNT greatly reduced background signals, thus resulting in contrast-enhanced imaging. The general applicability of the strategy was also testified by detecting Ramos cells with aptamer TD05. It was implied that F-apt/SWNT ensembles hold great potential as a simple, stable, sensitive, specific, and versatile activatable platform for both *in vitro* cancer cell detection and *in vivo* cancer imaging.

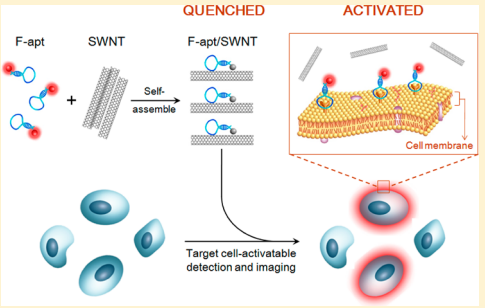

Nucleic acid aptamers are single-stranded RNA or DNA oligonucleotides with distinct binding properties to various targets including cancer markers and cells.[1−4] Having advantages of high affinity and specificity, low immunogenicity, fast tissue penetration, and uptake, as well as facile synthesis and modification, aptamers hold considerable promise as next-generation molecular probes for both *in vitro* and *in vivo* cancer diagnosis.[5,6] Currently, design of aptamer-based cancer detection probes primarily relies on an "always on" strategy, in which aptamers labeled with different reporters, such as radioactive, magnetic, and fluorescent agents, are bound to target cells and then result in an elevated signal around cells with reference to surroundings.[7−13] Due to the absence of signal alteration upon probe-target binding,[14,15] the *in vitro* utilization of "always on" probes typically requires a time-consuming washing step to eliminate interference from excessive unbound probes. For *in vivo* implementation, target specificity and imaging contrast may be compromised by a high background originating from constant signals in nontarget tissues.

As an alternative, "signal on" activatable aptamer probes (AAPs), in which normally quenched signals are activated only after targeting cancer cells, have been developed.[16−22] For example, several methods for direct cancer detection were reported by utilizing aggregation-induced signal enhancement of aptamer-modified gold nanoparticles (NPs) or magnetic NPs on target cell surface.[16−18] These assays serve as good candidates for *in vitro* cancer cell analysis with no required washing steps, but the relatively complex probe synthesis might impede their wide applications. Moreover, colorimetric signals of gold NPs are not applicable to *in vivo* imaging, and the need of expensive instrumentation may limit the popularity of magnetic methods. Our group previously designed a hairpin-structured AAP (HAAP) based on recognition-triggered conformational alteration, leading, in turn, to fluorescence restoration.[22] The HAAP not only achieved *in vitro* washing-free cancer cell analysis but also realized *in vivo* contrast-enhanced imaging. However, this probe still has shortcomings, such as low energy transfer efficiency between dyes and quencher molecules, indispensable sequence optimization, and susceptibility to nucleases attack in biofluids.[23] Hence, it is

Received: July 1, 2014
Accepted: August 25, 2014

   dx.doi.org/10.1021/ac5024149 | *Anal. Chem.* XXXX, XXX, XXX−XXX

urgently important to explore novel AAPs with ultralow background, high stability in biofluids, and good versatility for both *in vitro* and *in vivo* cancer cells.

Recently, carbon nanotubes (CNTs), a quasi one-dimensional nanomaterial with unique structural, mechanical, and optoelectronic properties, have become a popular star in biomedical and bioanalytical research.[24−29] In particular, the properties of long-range nanoscale energy transfer and biomolecule adsorption via π-stacking interaction make CNTs quite favorable for fluorometric assays.[30] Typical "signal on" biosensors based on dye-labeled aptamer-wrapped CNTs have been developed for detection of several analytes in the homogeneous phase, such as ATP, ochratoxin A, and thrombin.[31−33] But studies on complex and dynamic analytes like living cancer cells have not been reported yet.

Herein, we propose an activatable fluorescence probing platform for cancer cells based on self-assembled fluorophore-labeled aptamer/single-walled carbon nanotube (F-apt/SWNT) ensembles and present the first attempt to apply CNTs-based activatable probes in complex biological systems. As illustrated in Figure 1, cancer-targeted F-apts are adopted as

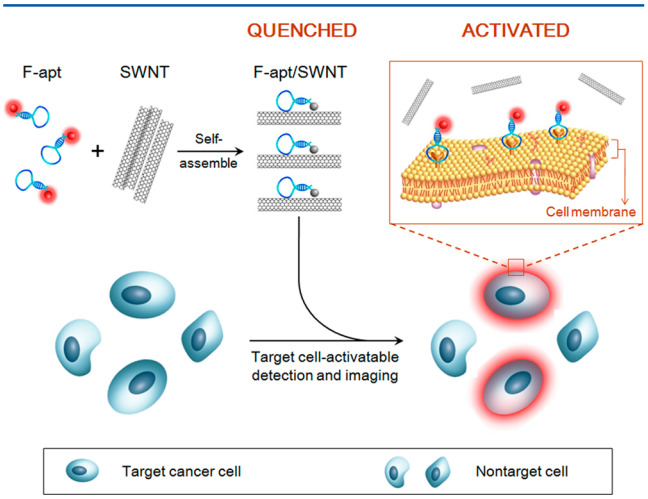

Figure 1. Schematic representation of the novel activatable fluorescence probing strategy for target cancer cells based on self-assembled fluorophore-labeled aptamer/single-walled carbon nanotube (F-apt/SWNT) ensembles.

recognition molecules, and SWNTs are utilized as both "nanoscaffolds" for aptamers and "nanoquenchers" of dyes. In free states, F-apts can self-organize on the surface of SWNTs, thus forming stable F-apt/SWNT complexes. And simultaneously, dyes are kept in close proximity to SWNTs with a quenched fluorescence obtained because of energy transfer. Whereas once F-apt/SWNT probes encounter target cancer cells, the specific binding of aptamers with protein receptors on the cell surface, which is stronger than the interaction between F-apts and SWNTs, can force F-apts to separate far from SWNTs. Thereupon, a fluorescence signal is activated in response to the presence of target cancer cells. As a "signal on" probe in combination with aptamers' high specificity, F-apt/SWNT ensembles may display low background and weak response to nontarget cells or proteins, thus offering a simple, fast, and direct cancer analysis in complex biofluids. Moreover, their fabrication mode of noncovalent self-assembly promises simplicity and generality. And the superquenching effect of SWNTs is expected to endow them much lower background and higher analytical sensitivity. Besides, SWNTs might also protect aptamers against nuclease digestion and thus improve their stability in biofluids for better performance.

EXPERIMENTAL SECTION

Materials and Reagents. All the DNA molecules reported in this article were custom-designed and then synthesized by Takara Biotechnology (Dalian) Co., Ltd. or Shanghai Sangon Biotechnology Co. Ltd. (Shanghai, China). Sequences of the oligonucleotides are listed in Table S-1. Single-walled carbon nanotubes (SWNTs) were purchased from Shenzhen Nanotech. Port Co. Ltd. Dulbecco's phosphate buffered saline with $CaCl_2$ and $MgCl_2$ (D-PBS) was obtained from Sigma. Mouse serum was purchased from WACAY. All other reagents were of the highest grade available. Deionized water was obtained through the Nanopure Infinity ultrapure water system (Barnstead/Thermolyne Corp.).

Oxidation and Characterization of SWNTs. The commercially purchased SWNTs were purified and oxidized according to the literature with some modifications.[31] First, 518.6 mg of SWNTs were refluxed in 100 mL of HNO_3 (2.0 M) for 1 day. Then, after centrifugation at 10 000 rpm for 30 min, the precipitate received an oxidation by 50 mL of a HNO_3/H_2SO_4 (1/3) mixture in an ultrasonic bath for 12 h at room temperature. Next, the oxidized SWNTs were centrifuged and washed with doubly distilled water to neutral pH. After treatment with a 0.22 μm filtration membrane to remove overlong SWNTs, the oxidized SWNTs were dried in an oven at 60 °C overnight, and finally stored in water at 1 mg/mL. Before the biological application, the as-prepared oxidized SWNTs were conventionally analyzed using transmission electron microscopy (TEM, JEOL-3010) and Fourier Transform infrared spectroscopy (FTIR, Tensor 27).

Preparation and Characterization of F-apt/SWNT Ensembles. F-apt/SWNT ensembles were formed based on the self-assembly behavior of F-apt molecules on SWNTs. Generally, F-apt molecules were mixed with SWNTs in D-PBS at a relatively high concentration. Then, the suspension was oscillated with a vortex shaker for 3 s. After incubation for 15 min at room temperature, the resulting F-apt/SWNT ensembles were ready for the subsequent use. The formation of F-apt/SWNT ensembles was determined on an F-2500 fluorescence spectrophotometer (Hitachi, Japan) by measuring the fluorescence signal of F-apt molecules. To investigate the fluorescence stability of F-apt/SWNT ensembles in complex biofluids, the fluorescence intensity variation vs time of different probes, including Cy5-Sgc8c, HAAP, and Cy5-Sgc8c/SWNT, was monitored at 37 °C in serum (excitation wavelength, 630 nm; emission wavelength, 664 nm). Moreover, the stability of different suspensions, including SWNTs before oxidation, SWNTs after oxidation, and Cy5-Sgc8c/SWNT, in different media such as water, D-PBS, and serum, was investigated by taking photographs with a digital camera after incubation for 2 h.

Cells. CCRF-CEM cells (T cell line, human acute lymphoblastic leukemia) were obtained from Cell Bank of the Committee on Type Culture Collection of the Chinese Academy of Sciences. Ramos cells (B cell line, human Burkitt's lymphoma) were purchased from the Cancer Institute & Hospital (Chinese Academy of Medical Sciences). CEN2 cells (human nasopharyngeal carcinoma, epithelioblastoma) and L02 cells (human normal hepatocyte) were obtained from the Shanghai Institute of Cell Biology of the Chinese Academy of

dx.doi.org/10.1021/ac5024149 | *Anal. Chem.* XXXX, XXX, XXX−XXX

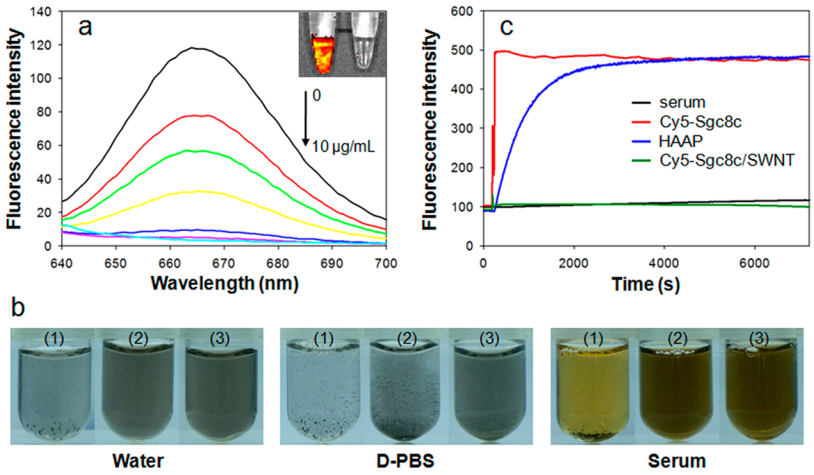

Figure 2. Characterization of F-apt/SWNT ensembles. (a) Fluorescence spectra of Cy5-Sgc8c (25 nM) with the addition of different concentrations of SWNTs. From top to bottom: 0, 1, 2, 3, 4, 5, and 10 μg/mL SWNTs, respectively. [Insets: images of Cy5-Sgc8c (25 nM) samples with (right) or without (left) addition of 10 μg/mL SWNTs, taken by a fluorescent imaging system.] (b) Photographs of different SWNTs samples in different media after incubation for 2 h. (1) SWNTs before oxidation; (2) SWNTs after oxidation; (3) Cy5-Sgc8c/SWNT ensembles. (c) Fluorescence stability of different probes at 37 °C in serum along with the extension of incubation time. (Cy5-Sgc8c and HAAP: 100 nM; SWNTs: 40 μg/mL).

Science. Cells were cultured in RPMI 1640 medium supplemented with 15% fetal calf serum (FBS), 100 mg/mL streptomycin, and 100 IU/mL penicillin, incubated at 37 °C in a humidified incubator containing 5 wt %/vol CO_2. The cell density was determined using a hemocytometer.

Flow Cytometry Assays. Generally, probes with different concentrations were incubated with 2×10^5 cells in 200 μL D-PBS on ice for 30 min in the dark and then immediately determined with a FACScan cytometer (BD Biosciences) by counting 10 000 events. For the detection of spiked serum samples, a similar procedure was conducted just with D-PBS replaced by serum. Regarding the sensitivity investigation of the Cy5-Sgc8c/SWNT strategy for CCRF-CEM cells analysis in mixed cell samples, the detailed protocol was somewhat modified. Briefly, mixed cell samples were prepared by using target CCRF-CEM cells and nontarget Ramos cells in D-PBS. The total cell number was fixed at 100 000, and thereinto CCRF-CEM cells varied from 0 to 25 000 cells. To exclude the interference from dead cells, cell samples were additionally stained with PI after incubation with Cy5-Sgc8c/SWNT (25 nM/10 μg/mL) for 30 min on ice in the dark. Then, cell samples were immediately detected with flow cytometer by counting 100 000 events.

Laser Scanning Confocal Microscopy Investigation. Mixed cell samples containing equivalent CCRF-CEM cells and Ramos cells were first incubated with a mixture of Cy5-Sgc8c/SWNT and FAM-TD05/SWNT in D-PBS on ice for 30 min in the dark, and then placed in a glass dish for observation on a laser scanning confocal microscope.

Animals. Male athymic BALB/c mice were purchased from the Shanghai SLAC Laboratory Animal Co., Ltd. All animal operations were in accord with institutional animal use and care regulations, according to protocol no. SYXK (Xiang) 2008−0001, approved by the Laboratory Animal Center of Hunan. Tumor-bearing animals were prepared through a subcutaneous injection of 5×10^6 *in vitro*-propagated cancer cells into the backside of nude mice. Tumors were then allowed to grow to 0.5−2 cm in diameter for 1−2 months.

***In Vivo* Fluorescence Imaging.** Before imaging, BALB/c nude mice, with or without tumors, were anesthetized with the combined use of tranquilizer and anesthetic. To test the feasibility of activatable imaging, tumor-bearing mice received an intratumoral injection of 100 μL D-PBS containing 5 pmol Cy5-DNA and 3 μg SWNTs. At certain time points, fluorescence images of live mice were taken by an IVIS Lumina II *in vivo* imaging system (Caliper LifeSicence, USA). The control normal mice received an intramuscular injection at a similar site where tumor grafted in tumor-bearing mice. Subsequently, time-lapse fluorescence imaging of CCRF-CEM tumor-bearing mice was performed after intravenous injection of 200 μL D-PBS containing 0.4 nmol Cy5-Sgc8c and 30 μg SWNTs. CCRF-CEM tumor-bearing mice intravenously injected with only 0.4 nmol Cy5-Sgc8c were imaged for comparison.

RESULTS AND DISCUSSION

Characterization of F-apt/SWNT Ensembles. To demonstrate feasibility of the F-apt/SWNT strategy for *in vitro* and *in vivo* cancer probing, Sgc8c, a DNA aptamer selected by cell-SELEX against human leukemia CCRF-CEM cells[1] and identified to specifically interact with cell membrane protein tyrosine kinase-7,[34] was chosen as a main model. Cy5-labeled Sgc8c (Cy5-Sgc8c) was designed to construct Cy5-Sgc8c/SWNT ensembles. In view of commercially purchased SWNTs' polydisperse micrometer lengths and weak stability for biological applications, they first received a purification and oxidation treatment before preparing Cy5-Sgc8c/SWNT probes. TEM and FTIR analysis results showed that the chemical oxidation effectively cut long SWNTs into short ones with lengths of 50−150 nm and obviously improved the dispersity of SWNTs by increasing oxygen-containing groups (Figure S-1). Subsequently, the oxidized SWNTs with different concentrations were used to interact with Cy5-Sgc8c. As displayed in Figure 2a, strong fluorescence was measured for the Cy5-Sgc8c solution without SWNTs. After the addition of SWNTs, the fluorescence signal of Cy5-Sgc8c was evidently reduced. And with the concentration of SWNTs increased, a gradual signal decrease was observed. As the concentration of SWNTs was elevated to 10 μg/mL, the quenching efficiency was estimated to be over 97%. It was indicated that the oxidized SWNTs could be effectively utilized as both "nanoscaffolds"

dx.doi.org/10.1021/ac5024149 | *Anal. Chem.* XXXX, XXX, XXX−XXX

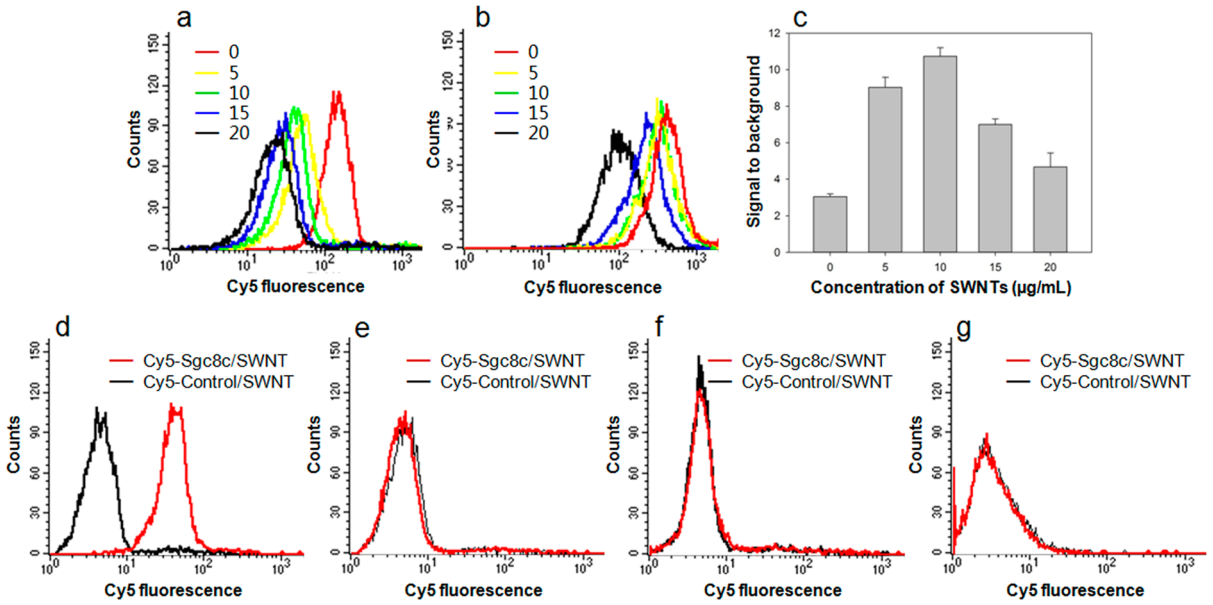

Figure 3. Feasibility investigation of the F-apt/SWNT strategy for target cancer cell detection. (a, b) Concentration optimization of SWNTs through flow cytometry assays of target CCRF-CEM cells after incubation with Cy5-Control/SWNT (a) or Cy5-Sgc8c/SWNT (b). (Cy5-DNA: 25 nM; SWNTs: 0−20 μg/mL.) (c) The corresponding histogram of the fluorescence ratios of Cy5-Sgc8c/SWNT to Cy5-Control/SWNT for labeling CCRF-CEM cells. (Error bars represent standard deviations from three repeated experiments.) (d−g) Flow cytometry assays of CCRF-CEM cells (d), Ramos cells (e), CEN2 cells (f), and L02 cells (g) after incubation with Cy5-Control/SWNT or Cy5-Sgc8c/SWNT by counting 10 000 events. (Cy5-DNA: 25 nM; SWNTs: 10 μg/mL.)

and "nanoquenchers" for constructing AAPs, and Cy5-Sgc8c/SWNT ensembles with ultralow background signals could facilely form via the self-assembly effect and proximity-induced energy transfer.

As an essential property to biological applications, the stability of Cy5-Sgc8c/SWNT ensembles in different media was tested in comparison with SWNTs before and after oxidation. Results in Figure 2b revealed that after incubation for 2 h, SWNTs before oxidation strongly aggregated and precipitated no matter in water, D-PBS, or serum. Through oxidation, SWNTs were stable in both water and serum, but an obvious aggregation in D-PBS was still observed. In contrast, due to the possibility of the wrap of DNA molecules effectively improving the stability of SWNTs,[35] Cy5-Sgc8c/SWNT ensembles held a much better dispersity in all the three media, thus guaranteeing their efficacy for both *in vitro* and *in vivo* applications. A further investigation of the fluorescence stability of Cy5-Sgc8c/SWNT ensembles in complex biofluids, such as serum, was conducted in comparison with the previously developed fluorescent HAAP.[22] As shown in Figure 2c, as a DNA probe, HAAP might be rapidly degraded by nucleases in serum, thus exhibiting a gradual elevation of its fluorescent signal from quenched to eventually equivalent to the "always on" Cy5-Sgc8c probe within ∼1 h. However, Cy5-Sgc8c/SWNT ensembles exhibited much better fluorescence stability. The fluorescent signal did not obviously change within ∼2 h and maintained a quenched effect throughout the monitoring process. It was demonstrated that the self-assembled Cy5-Sgc8c/SWNT was extremely stable even in complex biofluids at 37 °C, and SWNTs might effectively protect surface Cy5-Sgc8c molecules from the nuclease attack and the nontarget molecule interference. This provides a substantial basis for Cy5-Sgc8c/SWNT ensembles as an activatable fluorescence probing strategy with low background and high sensitivity in complex systems.

Specific Activation of F-apt/SWNT Ensembles by Target Cancer Cells. Flow cytometry assays were performed to investigate the fluorescence activation of F-apt/SWNT ensembles by target cancer cells. Cy5-Control, a negative control probe for Cy5-Sgc8c, was constructed with an arbitrary sequence alteration such that it showed little affinity to target CCRF-CEM cells. Correspondingly, Cy5-Control/SWNT was used as the control probe for Cy5-Sgc8c/SWNT. Figure 3a−c depicts the fluorescence signals of Cy5-Sgc8c/SWNT and Cy5-Control/SWNT, consisting of 25 nM Cy5-DNA and various concentrations of SWNTs, in response to CCRF-CEM cells. After incubation with CCRF-CEM cells, Cy5-Control/SWNT displayed decreased background responses with increased SWNTs concentration. On the other hand, with lower SWNTs concentration, the resulting signal of Cy5-Sgc8c/SWNT activated by target CCRF-CEM cells was higher. The signal-to-background ratios (S/B) of Cy5-Sgc8c/SWNT to Cy5-Control/SWNT for labeling CCRF-CEM cells are given in Figure 3c. The best S/B was detected as high as ∼11, which was achieved using 10 μg/mL SWNTs and greatly enhanced to ∼3.5 times of the "always on" Cy5-Sgc8c probe (without SWNTs). By further investigating the effect of incubation time on S/B, 30 min-incubation of CCRF-CEM cells with Cy5-Sgc8c/SWNT was optimized and used as a conventional condition in the following experiments (Figure S-2).

We next testified the specificity of the Cy5-Sgc8c/SWNT strategy for activatable detection of target CCRF-CEM cells by using several nontarget cell lines, including two cancer cell lines (Ramos cells and CEN2 cells), as well as one normal cell line (L02 cells). It was observed in Figure 3d that Cy5-Sgc8c/SWNT realized much higher labeling of CCRF-CEM cells than Cy5-Control/SWNT, revealing a substantial activation of Cy5-Sgc8c/SWNT after binding with membrane proteins of target cancer cells with an elevated fluorescence. In contrast, fluorescence responses of Cy5-Sgc8c/SWNT to three control

dx.doi.org/10.1021/ac5024149 | *Anal. Chem.* XXXX, XXX, XXX−XXX

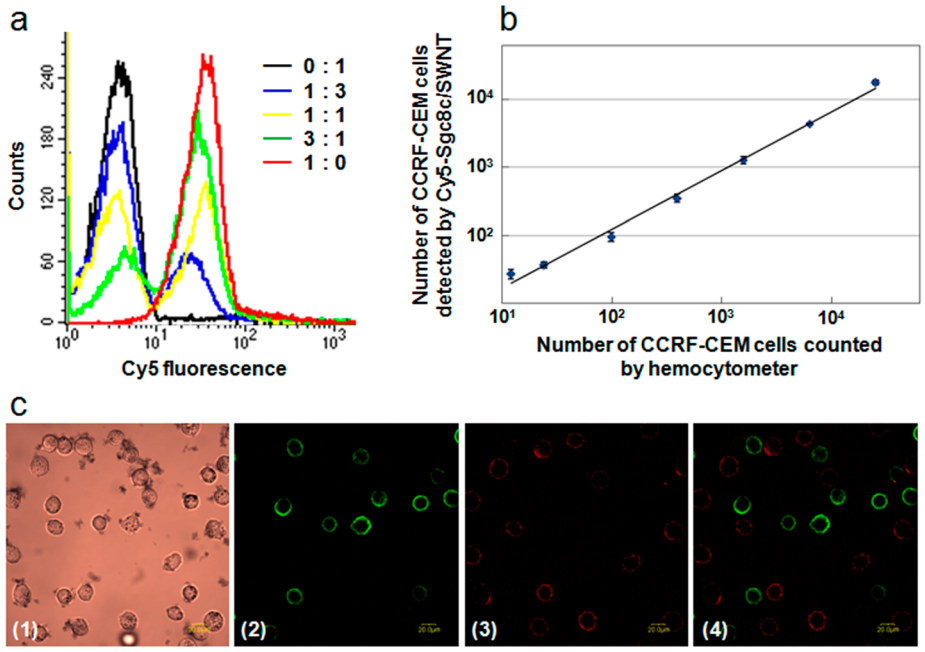

Figure 4. Detection of target cancer cells in mixed cell samples with the F-apt/SWNT strategy. (a) Flow cytometry assays of mixed cell samples with different concentration ratios of CCRF-CEM cells to Ramos cells using Cy5-Sgc8c/SWNT by counting 30 000 events. (Cy5-Sgc8c: 25 nM; SWNTs: 10 μg/mL.) (b) Calibration curve illustrating relationship between the amount of CCRF-CEM cells in mixed samples counted by hemocytometer and the number of CCRF-CEM cells detected in mixed samples by flow cytometer using Cy5-Sgc8c/SWNT. (The total cell number in mixed samples was fixed at 100 000; error bars represent standard deviations from three repeated experiments.) (c) Laser sanning confocal microscopy images of the mixed cell sample containing equivalent CCRF-CEM cells and Ramos cells after incubation with a mixture of Cy5-Sgc8c/SWNT and FAM-TD05/SWNT. (Cy5-Sgc8c, 100 nM; FAM-TD05, 100 nM; SWNTs, 80 μg/mL.) (1) Bright-field image, (2) FAM fluorescence image, (3) Cy5 fluorescence image, (4) merged image of 2 and 3.

cell lines did not exhibit significant difference from those obtained with Cy5-Control/SWNT, thus demonstrating a failed activation of Cy5-Sgc8c/SWNT by nontarget cells (Figure 3e–g). It was implied that the Cy5-Sgc8c/SWNT strategy held the desired ability to work on cell membrane proteins, and the activation of the Cy5-Sgc8c/SWNT was critically dependent on protein expression patterns of cells.

Detection of Cancer Cells with F-apt/SWNT Ensembles. The specific Cy5-Sgc8c/SWNT strategy was then applied to analyze target CCRF-CEM cells in mixed samples containing different concentration ratios of CCRF-CEM cells to Ramos cells (Figure 4a). With the concentration ratio of CCRF-CEM cells to Ramos cells reduced from 3:1 to 1:3, the percentage of positive signals obtained using Cy5-Sgc8c/SWNT decreased accordingly from 73.37% to 25.59%. The result strongly supported that the Cy5-Sgc8c/SWNT strategy held high specificity to achieve the accurate detection of target cells even in mixed cell samples. Subsequently, a more systematic investigation was performed to inspect sensitivity of the Cy5-Sgc8c/SWNT strategy. Mixed cell samples of CCRF-CEM cells and Ramos cells, with total cell number fixed at 100 000 and varying CCRF-CEM cell numbers ranging from 12 to 25 000 in 200 μL D-PBS, were obtained by serial dilution. To quantify target cell number, statistical analyses were performed according to the Cy5-Sgc8c/SWNT-labeled events appearing in the R1 region (Figure S-3). As CCRF-CEM cell number decreased, the number of events located in the R1 region decreased accordingly. Counts less than background count plus three times standard deviation were considered to be negative. Background count was determined using the same procedure without the addition of CCRF-CEM cells. For each group of samples, the number of CCRF-CEM cells detected by Cy5-Sgc8c/SWNT, Y, was plotted versus that measured using hemocytometer, X, as shown in Figure 4b. The regression equation was $\log Y = 0.8627 \times \log X + 0.3732$ with the smallest CCRF-CEM cell number of 12 detected in the presence of numerous nontarget cells. Furthermore, flow cytometry assays of CCRF-CEM cells in serum were also conducted using the Cy5-Sgc8c/SWNT strategy. It was confirmed that although the surrounding environment was changed from D-PBS to serum, which was more complex and unstable for activatable probes, the fluorescence elevation was still detected as a result of the activated Cy5-Sgc8c/SWNT by CCRF-CEM cells (Figure S-4). And Cy5-Sgc8c/SWNT still showed ~2.6 times enhanced S/B than the "always on" Cy5-Sgc8c probe.

The above F-apt/SWNT-based assay allowed a simple implementation through 30 min incubation of F-apt/SWNT with cancer cell samples before detection, implying that F-apt/SWNT ensembles held considerable potential as a simple, rapid, sensitive, and specific strategy for *in vitro* cancer cell detection with no required washing step. To further inspect the versatility of the F-apt/SWNT strategy for other cancer cells, TD05, a specific aptamer against Ramos cells, was utilized to construct F-TD05/SWNT ensembles. Flow cytometry assays demonstrated that a facile substitution of TD05 for the Sgc8c sequence realized the successful application of the F-apt/SWNT strategy in Ramos cell detection (Figure S-5). And as shown in Figure 4c, after a simple incubation of a mixed cell sample containing equivalent CCRF-CEM cells and Ramos cells with a mixture of FAM-TD05/SWNT and Cy5-Sgc8c/SWNT, the simultaneous imaging of different cancer cells was achieved through laser scanning confocal microscopy. Ramos cells were evidently labeled with FAM-TD05, exhibiting green fluorescence circles. CCRF-CEM cells were effectively stained

dx.doi.org/10.1021/ac5024149 | *Anal. Chem.* XXXX, XXX, XXX–XXX

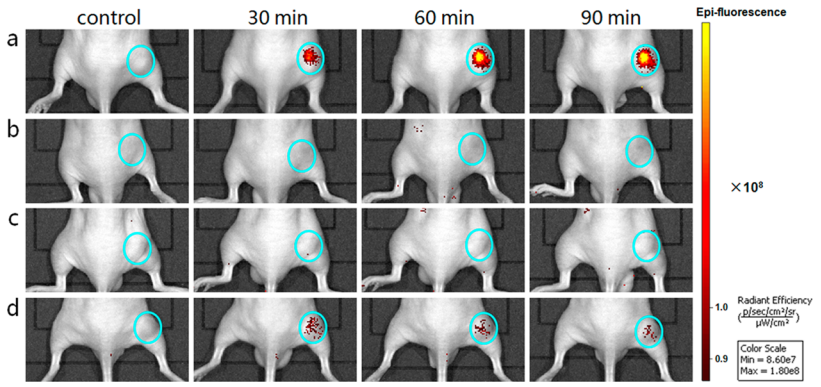

Figure 5. Time-lapse fluorescence imaging of living mice grafted with different tumors after intratumoral injection with different probes. (a) CCRF-CEM tumor-bearing mouse injected with Cy5-Sgc8c/SWNT. (b) Normal mouse without tumors injected with Cy5-Sgc8c/SWNT. (c) Ramos tumor-bearing mouse injected with Cy5-Sgc8c/SWNT. (d) CCRF-CEM tumor-bearing mouse injected with Cy5-Control/SWNT. (Cyan circles indicate the injection sites; The control image was taken before injection.)

by red fluorescence of Cy5-Sgc8c. In the whole imaging field, no cell was costained with both red and green fluorescence, thus proving the high specificity and low background of the F-apt/SWNT strategy once again.

***In Vivo* Contrast-Enhanced Cancer Imaging with F-apt/SWNT Ensembles.** We next implemented the developed F-apt/SWNT strategy for *in vivo* fluorescence imaging of target tumors implanted in nude mice. Figure 5 displays time-dependent *in vivo* fluorescence images of nude mice grafted with different tumors after intratumoral injection of different probes. As expected, under the same conditions, both the mouse without tumors and the Ramos tumor-bearing mouse did not show any obvious activated fluorescence within 90 min after the injection of Cy5-Sgc8c/SWNT (Figure 5b,c), which confirmed the extremely low background of Cy5-Sgc8c/SWNT even in real biological tissues. In contrast, prominent fluorescence signals began to appear in the CCRF-CEM tumor site just after injection of Cy5-Sgc8c/SWNT for 30 min and gradually enhanced with the postinjection time extended (Figure 5a). To further verify the above-detected fluorescence activation was triggered by specific binding of Cy5-Sgc8c to target cancer cells, a control experiment was performed by injecting Cy5-Control/SWNT into the CCRF-CEM tumor. As shown in Figure 5d, due to the weaker interaction between Cy5-Control and SWNTs, the nonspecific fluorescence was slightly brighter than other two control groups, but still much lower than signals from the CCRF-CEM tumor-bearing mouse injected with Cy5-Sgc8c/SWNT. This demonstrated that while its nonspecific activation was minimized, Cy5-Sgc8c/SWNT could be effectively activated by target tumors, thus affording a great potential for *in vivo* cancer imaging with enhanced contrast.

Then, a comparison between the Cy5-Sgc8c/SWNT strategy and the "always on" Cy5-Sgc8c strategy for *in vivo* cancer imaging was conducted using CCRF-CEM tumor-bearing mice. After intravenous injection of 200 μL D-PBS containing 0.4 nmol Cy5-Sgc8c, the mouse suffered high fluorescence background in the whole body from the earliest time point (Figure 6b). With the postinjection time prolonged, fluorescence signals faded gradually over the whole body including the tumor site. Because the binding of aptamers to target cancer cells might slow down their clearance in target tumor tissues, the tumor site was roughly distinguishable in fluorescence signals from nontarget sites with a very limited

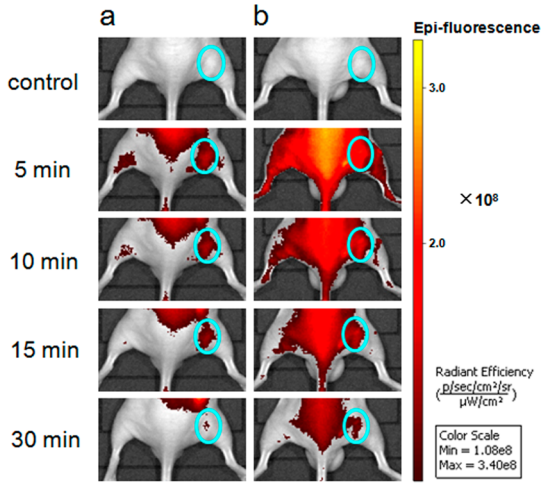

Figure 6. Time-dependent fluorescence imaging of CCRF-CEM tumor-bearing mice after intravenous injection with Cy5-Sgc8c/SWNT (a) and Cy5-Sgc8c (b). (The control image was taken before injection.)

signal-to-background ratio at 30 min. In contrast, a much lower fluorescence background was observed for the mouse intravenously injected with 200 μL of D-PBS containing Cy5-Sgc8c/SWNT (0.4 nmol/30 μg; Figure 6a). It is worth mentioning that in this experiment, the injection dose of SWNTs relative to Cy5-Sgc8c was greatly reduced in consideration of the potential toxicity of SWNTs to organisms, thus causing the background to not be removed fully. However, the tumor site could still be identified from nontarget sites with improved contrast after 5 min postinjection despite the signal interference from metabolic organs. With distinctly different behavior from Cy5-Sgc8c, Cy5-Sgc8c/SWNT could substantially minimize the background signal originating from nontarget tissues and display contrast-enhanced imaging within the 30 min investigation.

CONCLUSION

In this paper, a simple, stable, sensitive, specific, and versatile activatable platform for fluorescence probing of *in vitro* and *in vivo* cancer cells was developed based on self-assembled F-apt/SWNT ensembles. As a proof of concept, the Sgc8c aptamer against CCRF-CEM cells was used to construct Cy5-Sgc8c/SWNT with quenched fluorescence by utilizing SWNTs as

dx.doi.org/10.1021/ac5024149 | *Anal. Chem.* XXXX, XXX, XXX−XXX

both "nanoscaffolds" and "nanoquenchers." It was found that Cy5-Sgc8c could wrap and stabilize SWNTs in different media including water, D-PBS, and serum. And in return SWNTs might protect surface Cy5-Sgc8c from nuclease attack and nonspecific binding, thus endowing Cy5-Sgc8c/SWNT persistent ultralow background in serum. Subsequent *in vitro* assays confirmed that Cy5-Sgc8c/SWNT was specifically activated by target cancer cells and effectively improved sensitivity for detecting CCRF-CEM cells both in a buffer and serum. *In vivo* applications also demonstrated that in comparison with "always on" probes, Cy5-Sgc8c/SWNT achieved contrast-enhanced cancer imaging. Moreover, by introducing another aptamer TD05 for Ramos cells, the general applicability of the F-apt/SWNT strategy was realized. These results strongly support the F-apt/SWNT strategy as a versatile activatable fluorescence probing platform for *in vitro* and *in vivo* cancer cells with high specificity and sensitivity.

■ ASSOCIATED CONTENT

Supporting Information

Additional information as noted in text. This material is available free of charge via the Internet at http://pubs.acs.org.

■ AUTHOR INFORMATION

Corresponding Authors

*Tel/Fax: 86-731-88821566. E-mail: xiaoxiaohe@hnu.edu.cn.
*Tel/Fax: 86-731-88821566. E-mail: kmwang@hnu.edu.cn.

Author Contributions

†These authors contributed equally.

Notes

The authors declare no competing financial interest.

■ ACKNOWLEDGMENTS

This work was supported by the National Natural Science Foundation of China (Grants 21175039, 21190044, 21221003, 21322509, 21305035, and 21305038).

■ REFERENCES

(1) Shangguan, D.; Li, Y.; Tang, Z.; Cao, Z. C.; Chen, H. W.; Mallikaratchy, P.; Sefah, K.; Yang, C. J.; Tan, W. *Proc. Natl. Acad. Sci. U. S. A.* **2006**, *103*, 11838−11843.
(2) Liu, M.; Song, J.; Shuang, S.; Dong, C.; Brennan, J. D.; Li, Y. *ACS Nano* **2014**, *8* (6), 5564−5573.
(3) Li, X.; Zhang, W.; Liu, L.; Zhu, Z.; Ouyang, G.; An, Y.; Zhao, C.; Yang, C. J. *Anal. Chem.* **2014**, *86* (13), 6596−6603.
(4) Song, Y.; Zhu, Z.; An, Y.; Zhang, W.; Zhang, H.; Liu, D.; Yu, C.; Duan, W.; Yang, C. J. *Anal. Chem.* **2013**, *85*, 4141−4149.
(5) Fang, X.; Tan, W. *Acc. Chem. Res.* **2010**, *43*, 48−57.
(6) Tan, W.; Donovan, M. J.; Jiang, J. *Chem. Rev.* **2013**, *113*, 2842−2862.
(7) Liu, H.; Xu, S.; He, Z.; Deng, A.; Zhu, J.-J. *Anal. Chem.* **2013**, *85*, 3385−3392.
(8) Wu, Y.; Sefah, K.; Liu, H.; Wang, R.; Tan, W. *Proc. Natl. Acad. Sci. U. S. A.* **2010**, *107*, 5−10.
(9) Hicke, B. J.; Stephens, A. W.; Gould, T.; Chang, Y.-F.; Lynott, C. K.; Heil, J.; Borkowski, S.; Hilger, C.-S.; Cook, G.; Warren, S.; Schmidt, P. G. *J. Nucl. Med.* **2006**, *47*, 668−678.
(10) Zhang, C.; Ji, X.; Zhang, Y.; Zhou, G.; Ke, X.; Wang, H.; Tinnefeld, P.; He, Z. *Anal. Chem.* **2013**, *85*, 5843−5849.
(11) Shi, H.; Tang, Z.; Kim, Y.; Nie, H.; Huang, Y.; He, X.; Deng, K.; Wang, K.; Tan, W. *Chem.—Asian J.* **2010**, *5*, 2209−2213.
(12) Hwang, D. W.; Ko, H. Y.; Lee, J. H.; Kang, H.; Ryu, H. S.; Song, I. C.; Lee, D. S.; Kim, S. *J. Nucl. Med.* **2010**, *51*, 98−105.
(13) Medley, C. D.; Bamrungsap, S.; Tan, W.; Smith, J. E. *Anal. Chem.* **2011**, *83*, 727−734.
(14) Urano, Y.; Asanuma, D.; Hama, Y.; Koyama, Y.; Barrett, T.; Kamiya, M.; Nagano, T.; Watanabe, T.; Hasegawa, A.; Choyke, P. L.; Kobayashi, H. *Nat. Med.* **2009**, *15*, 104−109.
(15) Blum, G.; von Degenfeld, G.; Merchant, M. J.; Blau, H. M.; Bogyo, M. *Nat. Chem. Biol.* **2007**, *3*, 668−677.
(16) Medley, C. D.; Smith, J. E.; Tang, Z.; Wu, Y.; Bamrungsap, S.; Tan, W. *Anal. Chem.* **2008**, *80*, 1067−1072.
(17) Bamrungsap, S.; Chen, T.; Shukoor, M. I.; Chen, Z.; Sefah, K.; Chen, Y.; Tan, W. *ACS Nano* **2012**, *6*, 3974−3981.
(18) Lu, W.; Arumugam, S. R.; Senapati, D.; Singh, A. K.; Arbneshi, T.; Khan, S. A.; Yu, H.; Ray, P. C. *ACS Nano* **2010**, *4*, 1739−1749.
(19) Beqa, L.; Fan, Z.; Singh, A. K.; Senapati, D.; Ray, P. C. *ACS Appl. Mater. Interfaces* **2011**, *3*, 3316−3324.
(20) Yin, J.; He, X.; Wang, K.; Xu, F.; Shangguan, J.; He, D.; Shi, H. *Anal. Chem.* **2013**, *85*, 12011−12019.
(21) Cao, L.; Cheng, L.; Zhang, Z.; Wang, Y.; Zhang, X.; Chen, H.; Liu, B.; Zhang, S.; Kong, J. *Lab Chip* **2012**, *12*, 4864−4869.
(22) Shi, H.; He, X.; Wang, K.; Wu, X.; Ye, X.; Guo, P.; Tan, W.; Qing, Z.; Yang, X.; Zhou, B. *Proc. Natl. Acad. Sci. U. S. A.* **2011**, *108*, 3900−3905.
(23) Shi, H.; He, X.; Cui, W.; Wang, K.; Deng, K.; Li, D.; Xu, F. *Anal. Chim. Acta* **2014**, *812*, 138−144.
(24) Dai, H. *Acc. Chem. Res.* **2002**, *35*, 1035−1044.
(25) Liu, Z.; Davis, C.; Cai, W.; He, L.; Chen, X.; Dai, H. *Proc. Natl. Acad. Sci. U. S. A.* **2008**, *105*, 1410−1415.
(26) Ouyang, X.; Yu, R.; Jin, J.; Li, J.; Yang, R.; Tan, W.; Yuan, J. *Anal. Chem.* **2011**, *83*, 782−789.
(27) Welsher, K.; Liu, Z.; Daranciang, D.; Dai, H. *Nano Lett.* **2008**, *8*, 586−590.
(28) Guo, Y.; Shi, D.; Cho, H.; Dong, Z.; Kulkarni, A.; Pauletti, G. M.; Wang, W.; Lian, J.; Liu, W.; Ren, L.; Zhang, Q.; Liu, G.; Huth, C.; Wang, L.; Ewing, R. C. *Adv. Funct. Mater.* **2008**, *18*, 2489−2497.
(29) Liu, Z.; Sun, X.; Nakayama-Ratchford, N.; Dai, H. *ACS Nano* **2007**, *1*, 50−56.
(30) Yang, R.; Jin, J.; Chen, Y.; Shao, N.; Kang, H.; Xiao, Z.; Tang, Z.; Wu, Y.; Zhu, Z.; Tan, W. *J. Am. Chem. Soc.* **2008**, *130*, 8351−8358.
(31) Zhen, S. J.; Chen, L. Q.; Xiao, S. J.; Li, Y. F.; Hu, P. P.; Zhan, L.; Peng, L.; Song, E. Q.; Huang, C. Z. *Anal. Chem.* **2010**, *82*, 8432−8437.
(32) Guo, Z.; Ren, J.; Wang, J.; Wang, E. *Talanta* **2011**, *85*, 2517−2521.
(33) Yang, R.; Tang, Z.; Yan, J.; Kang, H.; Kim, Y.; Zhu, Z.; Tan, W. *Anal. Chem.* **2008**, *80*, 7408−7413.
(34) Shangguan, D.; Cao, Z.; Meng, L.; Mallikaratchy, P.; Sefah, K.; Wang, H.; Li, Y.; Tan, W. *J. Proteome Res.* **2008**, *7*, 2133−2139.
(35) Zheng, M.; Jagota, A.; Semke, E. D.; Diner, B. A.; Mclean, R. S.; Lustig, S. R.; Richardson, R. E.; Tassi, N. G. *Nat. Mater.* **2003**, *2*, 338−342.